arXiv:1508.03303v1 [math.NA] 13 Aug 2015

New insights on numerical error in symplectic integration *

August 14, 2015

Hugo Jiménez-Pérez*, Jean-Pierre Vilotte

Institut de Physique du Globe de Paris
1 rue Jussieu, 75865 Cedex Paris, France

Barbara Romanowicz[1,2,3]

[1] Institut de Physique du Globe de Paris
1 rue Jussieu, 75865 Cedex Paris, France
[2] Collège de France, Paris, France
[3] Department of Earth and Planetary Sciences
University of California, Berkeley, USA

Abstract

We implement and investigate the numerical properties of a new family of integrators connecting both variants of the symplectic Euler schemes, and including an alternative to the classical symplectic mid-point scheme, with some additional terms. This family is derived from a new algorithm, introduced in a previous study, for generating symplectic integrators based on the concept of special symplectic manifold. The use of symplectic rotations and a particular type of projection keeps the whole procedure within the symplectic framework.

We show that it is possible to define a set of parameters that control the additional terms providing a way of "tuning" these new symplectic schemes. We test the "tuned" symplectic integrators with the perturbed pendulum and we compare its behavior with an explicit $\mathcal{SAB}\mathcal{A}_2$ scheme for perturbed systems. Remarkably, for the given examples, the error in the energy integral can be reduced considerably. There is a natural geometrical explanation, sketched at the end of this paper. This is the subject of a parallel article where a finer analysis is performed. Numerical results obtained in this paper open a new point of view on symplectic integrators and Hamiltonian error.

*The first author is supported by a grant from the Fondation du Collège de France under the research convention PU14150472.

1 Introduction

A symplectic integrator for a Hamiltonian system is a numerical method which preserves the structure of the Hamiltonian vector field. Poincaré discovered that the flow of a Hamiltonian system forms a one-parameter subgroup of canonical transformations. In modern language, we say that the Hamiltonian flow is symplectic. The standard procedure for simulating Hamiltonian dynamics is by discretizing the Hamiltonian flow, which consists in discretizing the evolution time and looking for symplectic transformations which map the state of the system between two adjacent elements of the discretized time, e.g. from time t_n to time t_{n+1}.

It is well-known that one method for creating symplectic maps is based on generating functions, and it was already used by Poincaré when looking for periodic orbits of second genus [30]. In fact, generating functions were an important ingredient of the invariant integral theory pioneered by Poincaré and generalized by Cartan [4]. Since then, interest in generating functions remains very active from both the theoretical and the numerical point of view. Indeed for every symplectic transformation ψ there corresponds (at least locally) a class of functions generating a Lagrangian submanifold, i.e., the graph of a 1-form symplectomorphic to the Liouville form. In addition, Hamilton-Jacobi theory connects this Lagrangian submanifold with another submanifold invariant under the transformation ψ.

Lagrangian submanifolds used to obtain suitable maps for symplectic integrators must have a very particular form. They must contain all the information concerning the source and the target (symplectic) variables. This information, encoded in the Lagrangian submanifold, contains the well-known fact that generating functions for symplectic integrators must generate maps close to the identity. This criterion is not enough for determining whether the generating function associated to some symplectic map is suitable for obtaining a symplectic integrator. What is generally missing in the literature, is a geometrical approach distilling the theory behind the different techniques within a unified point of view on symplectic integrators. The present paper, together with [18, 15] are contributions in this direction. Before going over the theory, we briefly review previous results on symplectic integrators and generating functions related to the present paper.

The first article dealing with symplectic algorithms is attributed to De Vogelaere [38] in 1956. In 1983 Ruth [31] and Channell [5] made some progress with different techniques, in particular, Ruth pioneered explicit symplectic integrators and composition-splitting methods. Additional contributions were made independently by Menyuk [26] and Kang [19] in 1984. The same year, Kang Feng and his collaborators started a systematic study of symplectic integrators using generating functions [20, 13, 9]. His point of view was mostly algebraic, and based on Siegel's article [33], reprinted some years later in book format [34]. Some geometrization was achieved by Ge and Marsden [13], Ge [10, 11], Ge and Dau-liu [12], although their numerical algorithms were based on Feng's proce-

dure[1]. In 1990 Channell and Scovel [29] introduced symbolic computations to derive the integration formulas which arose in the procedure. Other important contributions were made by Sanz-Serna [32] who worked on symplecticity conditions for Runge-Kutta methods, and Miesbach and Pesch [27] who introduced some methods using Runge-Kutta techniques with generating functions. Many other authors have produced algorithms using generating functions, but the geometrical construction remains the same, and their contributions diverge from our discussion.

In a recent work [18], another link between generating functions for symplectic integrators and symplectic geometry has been studied, based on the concept of special symplectic manifold introduced by Tulczjyew in [40, 36]. Generating forms and functions in this framework were studied by Sniatycki and Tulczjyew [35] and Benenti [2, 3]. However, contributions from many other authors play a central role for the development and understanding of generating functions and their relationship with the Hamilton-Jacobi theory, such as Viterbo [37], Chaperon [6] Maslov [25], Hörmander [14], Weinstein [39] among many others.

In [18], the first author gives a strong argument for the construction of symplectic integrators based on the fact that solutions of the Hamilton-Jacobi equation for integrable and autonomous systems belong to a Lagrangian submanifold of the phase space [1]. Starting from the classical approach, the product manifold of two copies of the phase space is created in [18]. Then a generalized generating function with $4n$ variables is defined on the open ball of the product manifold centered at the initial condition (the source point of the map) and such that it contains the target point. The generating function is directly associated to a primitive 1-form on the product manifold considered as a special symplectic manifold on the configuration space. The problem is translated from looking for the generating function, to looking for the 1-form, also known as the *Liouvillian form* [28]. Two different Lagrangian submanifolds arise, one defined by the generating function, solution of the Hamilton-Jacobi equation, and the other invariant under the flow of the Hamiltonian vector field. Applying an analogous argument to the Hamilton's method of characteristics, the flow is searched in a transversal direction to the former submanifold. The suplementary space, transversal to the tangent space of the first Lagrangian submanifold, is projected by the induced projection[2], onto a $2n$ subspace, where the original Hamiltonian system is finally evaluated. The projection induces a family of one step implicit symplectic integrators of generic order 1[3], closely related to those already studied by Kang and co-workers and recently revisited by Xue and Zanna [41].

The main difference is that our numerical schemes contain some additional terms which vanish when the stepsize goes to zero. In particular, the symmet-

[1]Most of Feng's articles and some from his collaborators were recently edited in book format by M. Qin [21].

[2]The induced projection is the one we used to define the symplectic form on the product manifold by its pull-back.

[3]For some particular values of the parameters, we observe an increment in the order of convergence (see Figure 8).

ric integrators of the new family depend on $2n$ parameters and contain, as a special case, the midpoint rule. The goal of the present article is to perform a numerical study investigating those additional terms and their influence on the accuracy and performance. It is a numerically oriented paper; for the geometrical arguments and theoretical development we refer the reader to [18, 16]. More theoretical results related to the numerical error and the claim by Ge and Marsen [13, 11] about the impossibility of constructing exact numerical symplectic mappings is addressed in [15]. In fact, Ge's result [11] implies that our scheme should be exact up to numerical computer error and the residual error must be associated with the solution of the implicit equations.

2 Hamiltonian systems and Symplectic integrators

In what follows, we assume the reader is familiar with the terminology of differential geometry and vector bundles. For an introduction, the reader is referred to [1, 23, 24].

The approach presented in this work is based on the fact that Hamiltonian mechanics relies on the geometrical properties present in the evolution of a mechanical system which accepts a Hamiltonian description. For this reason, in this section we use the standard notation in modern symplectic geometry, topology and fiber bundles. The goal is to give a formal geometrical framework to study symplectic integrators as isometries of a generic symplectic form on generic symplectic manifolds. In this way, the construction of our symplectic methods takes a more abstract and general point of view solving, or correcting, some misunderstanding arising when the analysis is restricted to symplectic vector spaces, or cotangent bundles of linear spaces. In general, the starting point in symplectic integrator's analysis is the identification of a cotangent bundle with a symplectic vector space by the isomorphisms

$$T^*(\mathbb{R}^n) \overset{iso}{=} (\mathbb{R}^n)^* \oplus \mathbb{R}^n \overset{iso}{=} \mathbb{R}^{2n},$$

where $T^*(\mathbb{R}^n)$ is the cotangent bundle and $(\mathbb{R}^n)^*$ is the dual space of $\mathbb{R}^n$. However, this point of view hides the geometrical background of generating functions for constructing symplectic maps. Let us start with the main definitions and results.

A symplectic manifold is a $2n$-dimensional manifold M equipped with a non-degenerated, skew-symmetric, closed 2-form ω, such that at every point $m \in M$, the tangent space to M at m, denoted T_mM, has the structure of a symplectic vector space. One of the basic properties in symplectic geometry is given by Darboux's theorem which states that any symplectic manifold is locally symplectomorphic to a symplectic vector space (V, ω_0) with the canonical symplectic form $\omega_0(\cdot,\cdot) = \langle \cdot, J_0 \cdot \rangle$, where $\langle \cdot, \cdot \rangle$ is the canonical Euclidean structure

on V and J_0 is the almost complex structure represented by the matrix:

$$J_0 = \begin{pmatrix} 0_n & -I_n \\ I_n & 0_n \end{pmatrix}, \qquad 0_n, I_n \in M_{n\times n}(\mathbb{R}).$$

J_0 is also known as the canonical symplectic matrix on V. Consequently, the tangent space to M at m, with its symplectic form $\omega|_m = \omega_m$ and a suitable change of coordinates, can be completely described by the symplectic vector space with canonical symplectic coordinates $(\mathbf{x}, \mathbf{y}) \in V$, $y_i = J_0 x_i$. Darboux's theorem means that we systematically identify

$$(T_m M, \omega_m) \overset{iso}{=} (V, \omega_0), \qquad \forall m \in M,$$

selecting the right change of symplectic coordinates to describe the dynamics on M by the canonical symplectic coordinates $(\mathbf{x}, \mathbf{y}) \in V$.

Remark 1 *Unfortunately, Darboux's theorem hides a very rich environment suitable for investigating symplectic maps by use of generating functions and Liouvillian forms. In practice, it locally identifies all the symplectic manifolds of the same dimension with the cotangent bundle. The information about the symplectomorphism which maps the symplectic manifold of interest to the cotangent bundle is lost when we apply Darboux's theorem. To avoid this loss of information we stay in the generic geometric framework of symplectic geometry by using special symplectic manifolds.*

In this geometrical framework, a Hamiltonian system (M, ω, X_H) is a vector field $X = X_H$ on the symplectic manifold (M, ω) such that[4]

$$i_{X_H}\omega = -dH, \tag{1}$$

for a differentiable function $H : M \to \mathbb{R}$.

A natural diffeomorphism $\flat : TM \to T^*M$ between the tangent and the cotangent bundles of M is given by the contraction of the symplectic form with the vector field in the following way

$$X \mapsto \omega(X, \cdot).$$

The inverse of $\flat$ is denoted by $\sharp : T^*M \to TM$. Using $\sharp$, equation (1) is written in vector field form as

$$X_H = J\nabla H, \tag{2}$$

where ∇ is the standard gradient associated to the Euclidean structure. Expression (2) is best suited for applications. The equations of evolution can be written as

$$\dot{\mathbf{z}} = J\nabla_{\mathbf{z}} H(\mathbf{z}), \qquad \mathbf{z} \in M. \tag{3}$$

[4]Some authors write $i_{X_H}\omega = dH$ instead of (1), but it depends on the definition of ω as 2-form and the choice of the complex structure J.

Remark 2 *When $M = T^*\mathbb{R}^n$ is equipped with a canonical symplectic basis in cotangent coordinates $\mathbf{z} = (\mathbf{q}, \mathbf{p}) \in T^*\mathbb{R}^n$, the Hamiltonian vector field is given by Hamilton's equations:*

$$\dot{\mathbf{q}} = \frac{\partial H}{\partial \mathbf{p}}(\mathbf{q}, \mathbf{p}), \qquad \dot{\mathbf{p}} = -\frac{\partial H}{\partial \mathbf{q}}(\mathbf{q}, \mathbf{p}). \tag{4}$$

Poincaré discovered that the flow of any Hamiltonian vector field[5] is a 1-parameter subgroup of symplectic diffeomorphisms. Denoting such a flow by ϕ_H^t, this implies that for each fixed $h \in \mathbb{R}$, ϕ_H^h is a symplectic map.

Let $\mathbf{z}_0 \in M$ be a point on the symplectic manifold and $\mathbf{z}(t)$ the integral curve to X_H such that $\mathbf{z}_0 = \mathbf{z}(0)$. By definition of the flow, the mapping

$$\mathbf{z}(t + h) = \phi_H^h(\mathbf{z}(t))$$

will propagate the solution from time t to time $t + h$. A symplectic algorithm with stepsize h, is the numerical approximation ψ_h of the Hamiltonian flow $\phi_H^h : M \to M$, which is an isometry of the symplectic form ω . Specifically, consider the exact solution $\mathbf{z}(t)$ of a Hamiltonian system for the time $t \in [0, T]$, a discretization $\{t_i\}_{i=0}^N$ such that $t_0 = 0$, $t_N = T$, $h = T/N = t_{n+1} - t_n$, and denote $\mathbf{z}_n = z(t_n)$ for $0 \leq n \leq N$. Let $U \subset M$ be a convex open neighbourhood of $\mathbf{z}_n$ containing the target point $\mathbf{z}_{n+1}$.

With these hypotheses, we define a symplectic integrator as a map

$$\begin{aligned} \psi_h : U \subset M &\to U \\ \mathbf{z}_n &\mapsto \mathbf{z}_{n+1} = \psi_h(\mathbf{z}_n) \end{aligned}$$

smooth with respect to h and H, and such that $\psi_h^* \omega = \omega$, where ψ_h^* is the pullback of ψ_h defined by

$$(\psi_h^* \omega)_{\mathbf{z}}(\mathbf{v}, \mathbf{u}) = \omega_{\psi(\mathbf{z})}(T\psi_h(\mathbf{v}), T\psi_h(\mathbf{u})), \quad \mathbf{u}, \mathbf{v} \in T_z M. \tag{5}$$

Remark 3 *The vectors $T\psi_h(\mathbf{v})$ and $T\psi_h(\mathbf{u})$ belong to the tangent space $T_{\psi_h(\mathbf{z})}M$ which, in general, is different from $T_{\mathbf{z}}M$. Once we identify $\omega_{\mathbf{z}}$ and $\omega_{\psi_h(\mathbf{z})}$ with ω_0 and the tangent spaces $T_{\mathbf{z}}M$ and $T_{\psi_h(\mathbf{z})}M$ with V, condition (5) becomes*

$$\langle \mathbf{v}, J\mathbf{u} \rangle = \langle T\psi_h(\mathbf{v}), JT\psi_h(\mathbf{u}) \rangle.$$

or equivalently

$$\frac{\partial \psi_h}{\partial \mathbf{z}}^T J \frac{\partial \psi_h}{\partial \mathbf{z}} = J.$$

which is the well-known symplecticity condition for $\mathbb{R}^{2n}$ viewed as symplectic vector space. It is worth nothing that in the last expression, z are already local coordinates.

[5] Poincaré used the name of the "fundamental problem of dynamics", which is to find the solutions of the "fundamental equations of dynamics in canonical form" [30].

In an analogous way, we define an implicit symplectic integrator as a map

$$\begin{aligned} \varphi_h : U \times U &\to U \\ (\mathbf{z}_n, \mathbf{z}_{n+1}) &\mapsto \mathbf{z}_{n+1} = \varphi_h(\mathbf{z}_n, \mathbf{z}_{n+1}) \end{aligned}$$

smooth with respect to h and H, and such that $\varphi_h^* \omega = \omega$.

Since we are discretizing a flow, it is possible to consider an intermediate point $\bar{\mathbf{z}} \in U$ and two maps[6] $\psi_1, \psi_2 : U \to U$ such that $\bar{\mathbf{z}} = \psi_1(\mathbf{z}_n) = \psi_2(\mathbf{z}_{n+1})$. They let us rewrite the implicit scheme as $\varphi_h(\mathbf{z}_n, \mathbf{z}_{n+1}) = \psi_2^{-1} \circ \psi_1(\mathbf{z}_n)$.

The pullback becomes $\varphi_h^* \omega = (\psi_2^{-1} \circ \psi_1)^* \omega = \psi_1^* \circ (\psi_2^{-1})^* \omega$ which produces the corresponding symplecticity condition in the tangent spaces by

$$\left(\frac{\partial \psi_1^{-1}}{\partial \bar{\mathbf{z}}} \right)^T J \left(\frac{\partial \psi_1^{-1}}{\partial \bar{\mathbf{z}}} \right) = \left(\frac{\partial \psi_2^{-1}}{\partial \bar{\mathbf{z}}} \right)^T J \left(\frac{\partial \psi_2^{-1}}{\partial \bar{\mathbf{z}}} \right). \tag{6}$$

Note that on the left hand side of (6), J is an endomorphism on $T_{\mathbf{z}_n} U$ and on the right hand side, J is an endomorphism on $T_{\mathbf{z}_{n+1}} U$.

Condition (6) says nothing about the mappings ψ_1 and ψ_2, but only that the composition is a symplectic map. The reader interested is referred to [16] for a deeper discussion on conditions imposed on ψ_1 and ψ_2.

The discrete scheme ψ_h is said of order $r \in \mathbb{N}$ if, as $h \to 0$

$$\| \phi_H^h(\mathbf{z}_n) - \psi_h(\mathbf{z}_n) \| = \mathcal{O}(h^{r+1}), \qquad \mathbf{z}_n = \mathbf{z}(t_n) \in U.$$

There are several methods for constructing symplectic integrators that reduce to finding symplectic maps ϕ_H^h between two different (closed) points on the integral curves of the vector field X_H. Here we are interested in the method of generating functions that we describe in the next section.

3 Generating functions

It seems that Poincaré was the first author who systematically studied the process of obtaining symplectic maps by generating functions. However, the terminology was different in his work: Hamiltonian equations were called fundamental equations of dynamics in canonical form, symplectic maps were called canonical transformations[7]. Generating functions were the fundamental tool in his theory of integral invariants [30]. Poincaré used these transformations to study periodic orbits of second genus in celestial mechanics. It may explain why this technique was not acknowledged immediatelly by the numerical community. From the numerical point of view, generating functions for symplectic integrators were systematically studied by Feng's team in the mid '80s [19, 20, 8, 9] and later, among many others, by Ge and co-workers in late '80s and '90s [13, 10, 11, 12].

[6] In fact, they must be symplectic maps to have a consistent symplectic integrator [16].

[7] Transformations which preserves the canonical form of the fundamental equations of dynamics [30].

Both the analytical and the numerical procedures use the same framework that we outline now.

Let (M_1, ω_1) and (M_2, ω_2) be two symplectic manifolds of the same dimension. A map $\phi : M_1 \to M_2$ is called symplectic if $\phi^* \omega_2 = \omega_1$, where, in general ω_1 and ω_2 are different symplectic forms. In our case, $(M_1, \omega_1) = (M_2, \omega_2)$ are two copies of the same symplectic manifold, but we will preserve the subindices to keep record of what copy we refer to at every time.

Consider the product manifold $\tilde{M} = M_1 \times M_2$ with canonical projections $\pi_i : \tilde{M} \to M_i$ for $i = 1, 2$, and define a two-form $\omega_\ominus$ on $\tilde{M}$ by

$$\omega_\ominus \quad = \quad \pi_1^* \omega_1 - \pi_2^* \omega_2 \tag{7}$$

We have the following results (see [1, sec 5.2] for the proofs):

- $(\tilde{M}, \omega_\ominus)$ is a symplectic manifold of dimension $4n$.
- for any symplectic map $\phi : M_1 \to M_2$, the graph of ϕ, denoted by Γ_ϕ, and defined as

  $$\Gamma_\phi \quad = \quad \left\{ (\mathbf{z}, \phi(\mathbf{z})) \in \tilde{M} \mid \mathbf{z} \in M_1, \phi(\mathbf{z}) \in M_2 \right\},$$

  is a Lagrangian submanifold of $\tilde{M}$. This means $\omega_\ominus|_{\Gamma_\phi} = 0$
- Since $\theta_\ominus$ is a closed 1-form by the identity $d\theta_\ominus|_{\Gamma_\phi} \equiv 0$, using Poincaré's lemma, $\theta_\ominus$ is also an exact 1-form on Γ_ϕ. Then, there exists a function S defined on the Lagrangian submanifold Γ_ϕ such that its differential concides with the restriction of the 1-form $\theta_\ominus$ to Γ_ϕ

  $$S : \Gamma_\phi \to \mathbb{R}, \qquad \text{such that} \quad dS|_{\Gamma_\phi} \equiv \theta_\ominus|_{\Gamma_\phi}. \tag{8}$$

  $S : \Gamma_\phi \to \mathbb{R}$ is called a generating function for the symplectic map ϕ.

Symplectic maps, generating functions and Lagrangian submanifolds are closely related. For instance, in a generic symplectic manifold M, any Lagrangian submanifold $\Lambda \subset M$ which is transverse to the fibers of the projection $\pi_M : T^*M \to M$ can be locally parameterized by a suitable atlas of (local) functions S_i for short times [14, 25, 4]. Since symplectic integrators are mappings close to the identity (h small), we are not concerned with the global behaviour of the Lagrangian submanifolds and all our analysis will be local.

The standard procedure of the method of generating functions [19, 20] is as follows: 1) look for a suitable 1-form $\theta \in T^*\tilde{M}$ such that $d\theta = \omega_\ominus$; 2) obtain the Lagrangian submanifold $\Lambda \subset \tilde{M}$, associated with θ and a function $S : \Lambda \to \mathbb{R}$ satisfying $dS = \theta$; 3) solve the Hamilton-Jacobi equation on the Lagrangian submanifold; 4) design a numerical method for approximating such a solution giving the mapping $\mathbf{z}_{n+1} = \psi_h(\mathbf{z}_n)$ for $\mathbf{z}_n \in M_1$ and $\mathbf{z}_{n+1} \in M_2$.

Kang's procedure for solving the Hamilton-Jacobi equation is to approximate the generating function using Taylor series expansions [19]. Menyuk used the Picard iteration to obtain such a function [26] and Channell and Scovel used

symbolic computing software [29]. As pointed out by Miesbach and Pesch in [27], these approaches require higher order derivatives of the Hamiltonian which complicates the final scheme.

To keep the notation simple, from now on lowercase variables belong to M_1 and uppercase ones belong to M_2, in particular $\mathbf{z} = \mathbf{z}_n$ and $\mathbf{Z} = \mathbf{z}_{n+1}$. We use also Einstein notation in the definition of differential forms, i.e., $p_i dq_i := \sum_{i=0}^{n} p_i dp_i$.

3.1 The alternative method of Liouvillian forms

Recently, the first author made some contributions on the subject [18], where he avoids the solution of the Hamilton-Jacobi equation and recovers a numerical algorithm from geometrical interpretation of the solutions. Indeed, solutions of the Hamilton-Jacobi equation on the product manifold $\tilde{M}$, belong to a Lagrangian submanifold. This submanifold can be related to the characteristic bundle of the Hamiltonian vector field generated by a generalized generating function on $\tilde{M}$. The differential of this generalized function is actually a Liouvillian form, i.e. a 1-form λ on $\tilde{M}$ such that $d\lambda = \omega_{\ominus}$. A suitable projection $\pi : \tilde{M} \to N$ to a $2n$ dimensional submanifold $N \subset \tilde{M}$ gives the right point where we must evaluate the discrete flow in order to have a symplectic integrator. Contrasting this construction with Kang's procedure, we look for good values of the discrete flow on the Lagrangian submanifold defined by the Liouvillian form before the projection, instead of approximating the projection of the solution by Taylor series. Consequently, points 3) and 4) are not relevant in this construction. For more details the reader is referred to [18].

Our point of departure is the family of Liouvillian forms $\theta_{\alpha,\beta,\gamma}$ constructed in [18]. Consider two copies of the phase space $M_1 = T^*\mathcal{Q}_1$, $M_2 = T^*\mathcal{Q}_2$ and define the product manifold $\tilde{M} = M_1 \times M_2$ equipped with the 2-form $\omega_{\ominus}$ given in (7). As we know, $(\tilde{M}, \omega_{\ominus})$ is a symplectic manifold of dimension $4n$. Define local coordinates $(q_i, p_i) \in M_1$ and $(Q_i, P_i) \in M_2$, $i = 1, \cdots, n$, in each copy of the phase space and consider real numbers $\alpha, \beta, \gamma \in \mathbb{R}$. With this notation, the family of primitive 1-forms $\theta_{\alpha,\beta,\gamma}$ is given by

$$\begin{aligned} \theta_{\alpha,\beta,\gamma} &= \alpha(p_i dq_i + Q_i dP_i) - (1-\alpha)(P_i dQ_i - q_i dp_i) \\ &\quad +\beta(q_i dq_i + Q_i dQ_i) - \gamma(p_i dp_i + P_i dP_i), \end{aligned} \tag{9}$$

Since $\omega_{\ominus} = d\theta_{\alpha,\beta,\gamma}$ for any values of the parameters, we can give a full set of $3n$ different parameters $\{\alpha_i, \beta_i, \gamma_i\}_{i=0}^{n}$ for every 1-form $\theta_{\alpha,\beta,\gamma}$[8]. Note that the elements associated with β and γ belong to the kernel of the differential and they are known as the gauge elements of $\theta_{\alpha,\beta,\gamma}$. They do not modify the symplectic structure of $(\tilde{M}, d\theta_{\alpha,\beta,\gamma})$ but the solution in the Lagrangian submanifold will be, in general, different for each combination of parameters.

[8] The case $\beta_i = \gamma_i = \sqrt{\alpha_i(1-\alpha_i)}$ with $\alpha_i \in [0,1]$ corresponds to the family θ_{ϕ_i} constructed in [18] from the more elementary symplectic rotation $\alpha_i = \cos^2(\phi_i)$, $i = 1 \cdots, n$, on $\tilde{M} = M_1 \times M_2$.

Remark 4 *Every point $(\alpha_i, \beta_i, \gamma_i) \in \mathbb{R}^{3n}$, $i = 0, \cdots, n$, is associated to a 1-form whose differential is exactly the symplectic form $\omega_\ominus$. However, good values for a symplectic map approximating the Hamiltonian flow in a suitable way, belong to an open ball around the point $(\alpha_i, \beta_i, \gamma_i) = (1/2, 0, 0)$, associated to the mid-point symplectic map. In Section 4.1.2 we will find values for these parameters for a concrete example.*

All members of the family $\theta_{\alpha,\beta,\gamma}$ are 1-forms, locally closed on the graph $\Gamma_\phi \subset \tilde{M}$ of a generic symplectic map $\phi : (M_1, \omega_1) \to (M_2, \omega_2)$. By Poincaré's lemma, there exists a generating function $S = S_{\alpha,\beta,\gamma}$ depending on (α, β, γ) such that $dS = \theta_{\alpha,\beta,\gamma}$. The Lagrangian submanifold $\Lambda_{\alpha,\beta,\gamma}$ parameterized in local coordinates by the equation $dS = \theta_{\alpha,\beta,\gamma}$ has explicit form

$$\begin{aligned}
\frac{\partial S}{\partial q_i} &= \alpha p_i + \beta q_i && (10)\\
\frac{\partial S}{\partial p_i} &= -(1-\alpha) q_i - \gamma p_i && (11)\\
\frac{\partial S}{\partial Q_i} &= -(1-\alpha) P_i + \beta Q_i && (12)\\
\frac{\partial S}{\partial P_i} &= \alpha Q_i - \gamma P_i, && (13)
\end{aligned}$$

and must satisfy the homogeneous Hamilton-Jacobi equation $H(\Lambda_{\alpha,\beta,\gamma}) = 0$.

Consider a 2n-dimensional submanifold of the product manifold $N_{\alpha,\beta,\gamma} \subset \tilde{M}$ with coordinates $(\bar{Q}_i, \bar{P}_i)$, and define the projection $\pi_S : \tilde{M} \to N_{\alpha,\beta,\gamma}$ by

$$\pi_S = J \circ (\pi_1 - \pi_2)(\Lambda_{\alpha,\beta,\gamma}). \tag{14}$$

The submanifold $N_{\alpha,\beta,\gamma}$ is given in local coordinates by the equations

$$\begin{aligned}
\bar{Q}_i &= \alpha Q_i + (1-\alpha) q_i + \gamma (p_i - P_i)\\
\bar{P}_i &= \alpha p_i + (1-\alpha) P_i + \beta (q_i - Q_i). && (15)
\end{aligned}$$

Note that on the diagonal $\Delta_{\tilde{M}}$ of $\tilde{M}$ defined by

$$\Delta_{\tilde{M}} = \left\{ (q_i, p_i, Q_i, P_i) \in \tilde{M} \mid q_i = Q_i,\ p_i = P_i, \forall i = 1 \cdots n \right\},$$

the submanifold $N_{\alpha,\beta,\gamma}$ is a standard symplectic submanifold with the induced symplectic form ω_Δ which fulfils $\omega_\ominus = \pi_S^* \omega_\Delta$. Moreover, given the inclusion

$$\begin{aligned}
i : M &\to \tilde{M} && (16)\\
(q_i, p_i) &\mapsto (q_i, p_i, q_i, p_i) && (17)
\end{aligned}$$

whose image is exactly the diagonal $\Delta_{\tilde{M}} = i(M, \omega)$ we have $\omega = i^* \omega_\Delta$.

3.2 The implicit symplectic integrators

For $(\mathbf{z}, \mathbf{Z}) \in \tilde{M}$ where $\mathbf{z} = (q_i, p_i) \in M_1$ and $\mathbf{Z} = (Q_i, P_i) \in M_2$, the family of symplectic integrators given in [18] is obtained by the following implicit scheme[9]

$$\mathbf{Z} \quad = \quad \mathbf{z} + hJ\nabla H(T\pi_S(\mathbf{z}, \mathbf{Z})) \tag{18}$$

or in extended form

$$\begin{aligned} Q_i &= q_i + h\frac{\partial H}{\partial p_i}\left(\alpha Q_i + \alpha' q_i + \gamma(p_i - P_i), \alpha p_i + \alpha' P_i + \beta(q_i - Q_i)\right) \quad (19)\\ P_i &= p_i - h\frac{\partial H}{\partial q_i}\left(\alpha Q_i + \alpha' q_i + \gamma(p_i - P_i), \alpha p_i + \alpha' P_i + \beta(q_i - Q_i)\right) \end{aligned}$$

where we used $\alpha' = 1 - \alpha$ to simplify the expressions. We shall return to these expressions later, when we study the symmetric case. At this stage, it is worth to note that for $(\alpha, \beta, \gamma) = (0, 0, 0)$ and $(\alpha, \beta, \gamma) = (1, 0, 0)$, we obtain the staggered Euler symplectic integrators A and B [7]

$$Q_i = q_i + h\frac{\partial H}{\partial p_i}(q_i, P_i) \qquad Q_i = q_i + h\frac{\partial H}{\partial p_i}(Q_i, p_i) \tag{20}$$

$$P_i = p_i - h\frac{\partial H}{\partial q_i}(q_i, P_i) \qquad P_i = p_i - h\frac{\partial H}{\partial q_i}(Q_i, p_i) \tag{21}$$

The main remark on the choice of the method (18) is that projection π_S given in (14) is a "rearrangement" of the data coded in the Lagrangian submanifold $\Lambda_{\alpha,\beta,\gamma}$ in a close to symplectic submanifold $N_{\alpha,\beta,\gamma}$. This choice is rooted in the notion of geometrical solution to the Hamilton-Jacobi equation

$$\frac{\partial S}{\partial t} + H(\lambda) = 0$$

where the function $H : M \to \mathbb{R}$ of the Hamilton-Jacobi equation is evaluated on a Lagrangian submanifold $\lambda \subset M$ of a symplectic manifold (M, ω) given by local equations

$$\lambda = \left\{ (\mathbf{q}, \mathbf{p}) \in M \mid \mathbf{q} = \mathbf{q},\ \mathbf{p} = \frac{\partial S}{\partial \mathbf{q}} \right\},$$

and differs from the energy Hamiltonian function, only by a constant (normally denoted by $-E$). For the non-evolutionary Hamilton-Jacobi equation, considering the characteristic bundle, we evaluate the Hamiltonian vector field on the sub-bundle $(T\lambda)^{\perp} \subset TM$ transversal to $T\lambda$. An example is provided by the staggered Euler integrator of type A, with the difference approximation

$$\mathbf{Z} \quad = \quad \mathbf{z} + hJ\nabla H(\mathbf{Q}, \mathbf{p}), \tag{22}$$

of the differential equation $\dot{\mathbf{z}} = J\nabla H(\mathbf{Q}, \mathbf{p})$ associated to the Hamilton Jacobi equation $H(\mathbf{q}, \mathbf{P}) = 0$ for $\mathbf{z} = (\mathbf{q}, \mathbf{p})$ and $\mathbf{Z} = (\mathbf{Q}, \mathbf{P})$.

[9] Note that the projection (14) with local coordinates (15) is linear in (q_i, p_i, Q_i, P_i) and consequently it coincides with its linearization $T\pi_S$.

4 Numerical examples

All the members of the family (20) for which $\alpha \in (0,1)$ produce implicit symplectic integrators that we can compute in an iterative predictor-corrector scheme.

For the tests, we consider the perturbed Hamiltonian pendulum as toy example. The algorithm was implemented in python for testing the accuracy of the method and compared with the explicit method $\mathcal{SABA}_2$ with coefficients

$$\{a_0 = a_2 = 1/6, b_0 = b_1 = 1/2, a_1 = 2/3\},$$

studied by Laskar and Robutel in [22]. We used the staggered symplectic Euler integrator as predictor and we compute, iteratively, the intermediate coordinates $\bar{\mathbf{z}} = (\bar{\mathbf{Q}}, \bar{\mathbf{P}})$ which are used to compute the value of $\mathbf{z}_{n+1} = (\mathbf{p}_{n+1}, \mathbf{q}_{n+1})$ in κ iterations.

The general structure of the algorithm is the following

Algorithm 1.

!Setup the predictor
$\mathbf{z}^{[0]} = \mathbf{z}_n + hJ\nabla H(\mathbf{z}_n)$
for $j = 0 : \kappa$ do
  !compute the point $\bar{\mathbf{z}} = (\bar{\mathbf{Q}}, \bar{\mathbf{P}})$
  $\bar{\mathbf{Q}} = \alpha\mathbf{q}^{[j]} + (1-\alpha)\mathbf{q}_n + \gamma(\mathbf{p}_n - \mathbf{p}^{[j]})$
  $\bar{\mathbf{P}} = \alpha\mathbf{p}_n + (1-\alpha)\mathbf{p}^{[j]} + \beta(\mathbf{q}_n - \mathbf{q}^{[j]})$.
  !compute the corrector
  $\mathbf{z}^{[j+1]} = \mathbf{z}_n + hJ\nabla H(\bar{\mathbf{z}})$
end for
$\mathbf{z}_{n+1} = \mathbf{z}^{[\kappa]}$

4.1 The simple Hamiltonian pendulum

The simple Hamiltonian pendulum obeys the Hamiltonian equation

$$H(p,q) \quad = \quad \frac{1}{2}p^2 - \epsilon\cos q \tag{23}$$

where we have fixed $\epsilon = 0.03$. We performed several tests for different values of (α, β, γ) and the step size h. The total number of steps N used in the simulations was variable but almost all the results used $N = 10^5$.

A full set of generic parameters (α, β, γ) for our symplectic integrators in a Hamiltonian system with n degrees of freedom, has $3n$ elements. We are interested in some particular cases and the dimension of the space of parameters is different for each one. Since it is not evident in a 1 degree of freedom problem, we enumerate the dimension of the space of parameters for the cases used in the tests: 1) the case $(\alpha = 0.5, \beta = 0, \gamma = 0)$ has null dimension (is a point); 2) the case $(\alpha, \beta, \gamma = \beta)$ has dimension $2n$; 3) the case $(\alpha, \beta = \sqrt{\alpha(1-\alpha)}, \gamma = \sqrt{\alpha(1-\alpha)})$ has dimension n; 4) the case $(\alpha = 0.5, \beta = \sqrt{\alpha(1-\alpha)}, \gamma = \sqrt{\alpha(1-\alpha)})$ has null dimension, it is the point $(0.5, 0.5, 0.5)$; 5) the case $(\alpha = 0.5, \beta, \gamma)$ has dimension $2n$. Below the reader will see that we look for optimal values of β and γ in an open ball centered at the origin of $\mathbb{R}^{2n}$.

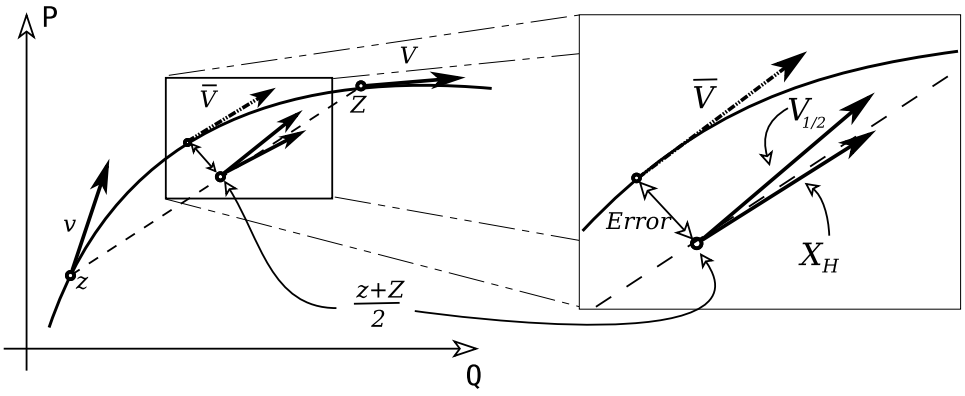

Figure 1: A simple illustration of the natural error obtained by the symplectic mid-point rule. In this plot we assume known the vectors $v = X_H(\mathbf{z}) = \dot{\mathbf{z}}$ and $V = X_H(\mathbf{Z}) = \dot{\mathbf{Z}}$ and we try to approximate $\bar{V}$ by computing $X_H\left(\frac{\mathbf{z}+\mathbf{Z}}{2}\right)$. Note that it coincides with $V_{\frac{1}{2}} = \frac{1}{2}(v+V)$ only if X_H is a linear vector field. Moreover, it coincides with $\bar{V}$ only when the solution $\mathbf{z}(t)$ is linear in t, or equivalently when X_H is constant.

4.1.1 Preliminary tests

We consider the classical symplectic mid-point rule as starting point since it is the algorithm corresponding to $(\alpha, \beta, \gamma) = (0.5, 0., 0.)$. The error associated to this case is easy to understand if we consider the projection of the orbit on the phase space (Figure 1). What we are looking for is some point $\bar{\mathbf{z}}$, as close as possible to the real orbit, such that on it, the real vector field is parallel to the numerical value. Of course, the point $\bar{\mathbf{z}}$ coincides with the mid point $\frac{1}{2}(\mathbf{z}_n + \mathbf{z}_{n+1})$ when the Hamiltonian vector field is constant.

When computing the symplectic mid-point rule with five iterations in the resolution of the implicit scheme, and comparing with the explicit integrator $\mathcal{SABA}_2$ from [22], we found that the former is more accurate for the selected set of initial conditions (upper-right plot in Figure 4). However, it is significantly more costly because it is an iterative scheme.

With this error reference's framework, we consider the case where (α, β, γ) are given by the simple symplectic rotation in [18]. The rotation corresponds to the parameters $\beta = \gamma = \sqrt{\alpha(1-\alpha)}$ for $\alpha \in [0, 1]$. The relevant observations follow:

a) Variations in α from 0 to 1 result in a progressive deformation of the orbit which connects consistently the symplectic Euler methods A with B. The energy is well conserved with the well-known oscillations for Euler methods. The oscillations are of the same order of magnitude for every member of the family. In the symmetric case $(\alpha, \beta, \gamma) = (0.5, 0.5, 0.5)$, the oscillations are really large compared with the mid-point case $(\alpha, \beta, \gamma) = (0.5, 0., 0.)$ (Figure 2).

b) Tests for stepsizes h between 0.001 and 0.1 exhibit a good behaviour and

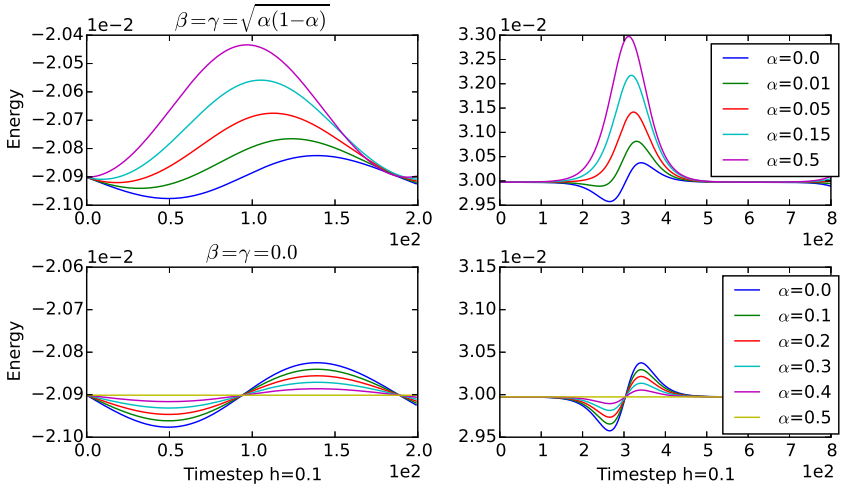

Figure 2: Oscillations around the energy integral of the numerical solutions computed with the new implicit method. Left column corresponds to initial condition $(q_0, p_0) = (0.8, 0.0)$ and $(q_0, p_0) = (3.1, 0.0)$ for the right column. Different graphs in each panel correspond to the solution varying from $\alpha = 0.0$ to $\alpha = 0.5$. Above: progresive deformation of the oscillations for the rotation $\beta = \gamma = \sqrt{\alpha(1-\alpha)}$. Below: the case $\beta = \gamma = 0.0$.

some deformation in the orbits is detected for $0.2 < h < 0.8$ and $\beta = \gamma = \sqrt{\alpha(1-\alpha)}$ (see right panel in Figure 3). For $h \geq 1.0$ the orbits experienced high oscillations and for initial conditions close to the hyperbolic fixed points the numerical solution went to the unbounded region. Deformation of the orbits in phase space corresponds to the oscillation of the numerical solution of the energy integral around the exact constant value of H. On the other hand, for small values of β and γ the numerical solutions has a good behaviour (see left panel in Figure 3) and some tests for $h = 10$ are really satisfactory.

The main remark from these preliminary tests is that parameters β and γ let us control the numerical error in the energy integral, and that values of the parameters close to $(\alpha, \beta, \gamma) = (0.5, 0, 0)$ have very small error. In the rest of the discussion we fixed $\alpha = 0.5$ and we considered small values for the other parameters. This value for α is strategic since α controls the symmetry of oscillations around the constant energy for positive and negative directions in time. This is evident from the well-known fact that symplectic methods are reversible in time if and only if they are symmetric. Moreover, oscillations for $\alpha \in (0, \frac{1}{2})$ when $\beta = \gamma = \sqrt{\alpha(1-\alpha)})$ in positive time (α, t), are symmetric with respect to those for $(1-\alpha, -t)$ in negative time.

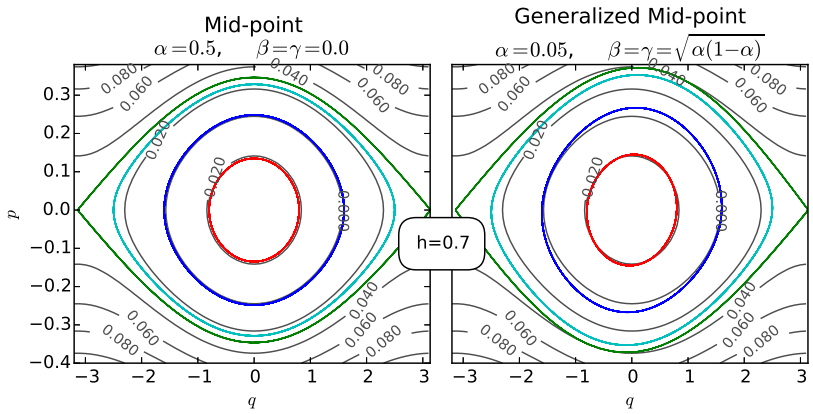

Figure 3: Orbits of the numerical solution for the perturbed Hamiltonian pendulum. We compare two different members of the family of implicit integrators $(\alpha, \beta, \gamma) = (0.5, 0, 0)$ and $(\alpha, \beta, \gamma) = (0.1, 0.3, 0.3)$ vs. the exact solution. There are four orbits in each plot, with initial conditions $(q_0, p_0) \in \{(0.8, 0.), (1.6, 0.), (2.5, 0.), (3.13, 0.)\}$, stepsize $h = 0.7$ and $k = 5$. Note the deformation of the orbits at the right panel.

4.1.2 The symmetric case $\alpha = 0.5$

We perform this analysis in two separate cases: the first one when γ is free and $\beta = \gamma$, and the second one when both β and γ are independent.

a) Let us fix $\alpha = 0.5$ and $\beta = \gamma$, with $\gamma \in [-0.5, 0.5]$. In this case, the amplitude of the oscillations in the energy goes from a positive to a negative phase (upper-left panel in Figure 4). Moreover, for $\gamma \sim 0$ and five iterations (for solving the implicit scheme) the amplitude of the oscillations is lower than oscillations of $\mathcal{SABA}_2$ with a better behavior (lower-left panel in Figure 4). This fact is remarkable since our implicit symplectic integrator is a one step method. Moreover the tests on the behaviour of the error with respect to the stepsize show a better accuracy than $\mathcal{SABA}_2$ (lower-right plot in Figure 4).

A finer analysis for different orbits with initial conditions close to one of the hyperbolic fixed points gives us new insight for the understanding of our numerical scheme.

b) Fix $\alpha = 0.5$ and consider independent values for $\beta, \gamma \in [-0.5, 0.5]$. We observe in this case, that each one of the parameters controls a different part of the oscillation around the energy integral. To show that, we choose an initial condition close to one hyperbolic fixed point. In an oscillation of a numerical solution given by a symmetric symplectic method (for instance $\mathcal{SABA}_2$), three cusps arise[10]. In our results, β controls the central cusp in a very clear and definite way. This property is shown in the upper row of Figure 5. In this plot

[10] We need to check if other methods and other Hamiltonian problems behave in a similar way.

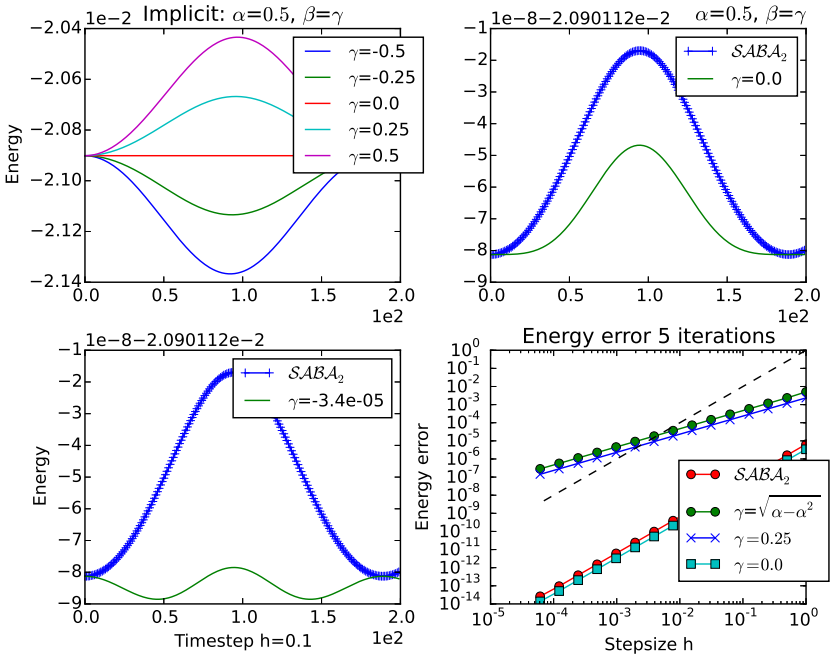

Figure 4: Comparison of the oscillations of the numerical solution around the constant energy integral, between the new integrator with $\alpha = 0.5$ and the explicit $\mathcal{SABA}_2$ integrator. All plots have initial condition $(q_0, p_0) = (0.8, 0.0)$, the stepsize in the three plot of energy integrals is $h = 0.2$. Above-left: variation of the $\beta = \gamma$ parameters in $\{-0.5, -0.25, 0, 0.25, 0.5\}$ Above-right: new method for $\beta = \gamma = 0$ wompared to $\mathcal{SABA}_2$. Below-left: minimal oscillation around the energy integral of the new method for $\beta = \gamma = -3.4 \times 10^{-5}$. Below-right: generic members of the family have order 1. The dotted line corresponds to h^2.

we fixed $\gamma = -00.7$ and we modified β visually such that the cusp be close to the constant energy. Then, we fix β and modify γ, which controls the two cusps until we arrive at a very flat solution as we can see in the lower panel in Figure 5.

By a continuity argument we search for optimal values of β and γ, reducing the error in the numerical solution. This is done as a manual and visual process, computing the maximum variation of the error within an open square around $(\beta, \gamma) = (0, 0)$. We obtain a well defined region where such values belong. Maximum variation in the energy integral for the perturbed Hamiltonian pendulum, with initial conditions $(q_0, p_0) = (3.1, 0.0)$, stepsize $h = 0.1$, perturbing term $\epsilon = 0.03$ and $k = 5$ iterations went to $err < 5 \times 10^{-14}$, which is remarkable for a one step integrator. Figure 6 shows the maximum variation of the error for a

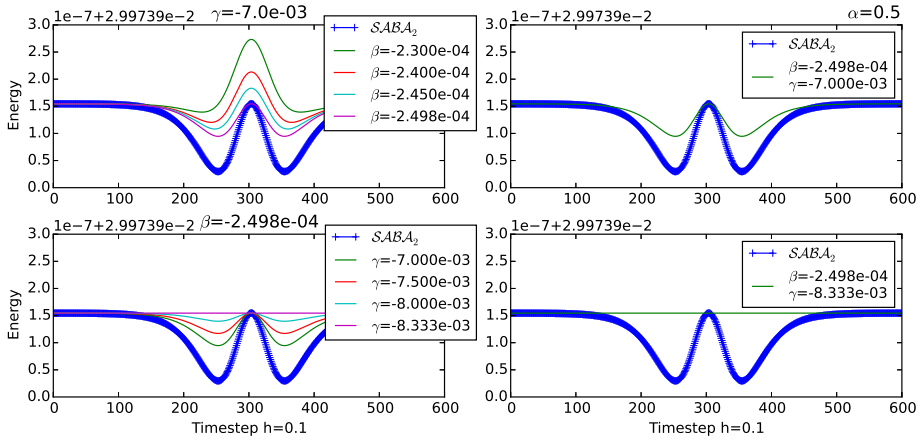

Figure 5: Search of optimal values for β and γ with $\alpha = 0.5$. Above: variation of the β parameter changes the position of the central cusp. Below-left: variation of the γ parameter changes the position of the sourounding cusps. Below-right: an optimal combination of parameters β and γ reducing the error oscillations around $err < 10^{-13}$. See left panel in Figure 6 for a zoomed version of this plot. The fixed oscillating orbit corresponds to the numerical solution of the $\mathcal{SABA}_2$ integrator. All plots have initial condition $(q_0, p_0) = (3.1, 0.0)$ and stepsize $h = 0.1$.

subset of $\mathbb{R}^2$ and the computed numerical energy compared with $\mathcal{SABA}_2$. The vertical line in the middle of the left panel in Figure 6 is the central cusp of the $\mathcal{SABA}_2$ integrator. It is a zoomed version of the lower-right panel from Figure 5.

4.1.3 Interpretation of the parameters β and γ

The fact that the new parameters β and γ control the numerical error is an important result. However, the way we obtained these values is quite heuristic. In order for these parameters to be really advantageous, their behaviour with respect to the variations in the stepsize h must be investigated.

To check their dependency on the stepsize h, we performed several tests with the same initial conditions as in the previous tests. We searched for the optimal values of β and γ for $h \in \{0.05, 0.1, 0.5, 1.0\}$ and we obtained an almost perfect linear relationship $\beta = h \cdot b$ and $\gamma = h \cdot c$ for $b = -2.4978136594 \times 10^{-3}$ and $c = -8.33321735568 \times 10^{-2}$ (see upper row and lower-right panel in Figure 7). To verify the linear dependence, we extrapolated and interpolated several values of the parameters for different h. The linear relationship holds in a very accurate way. The lower-right panel in Figure 7 is computed with the extrapolated parameters for $h = 0.007$. Figure 8 shows the values found by visual inspection for $h \in \{0.05, 0.1, 0.5, 1.0\}$ and the line joining them.

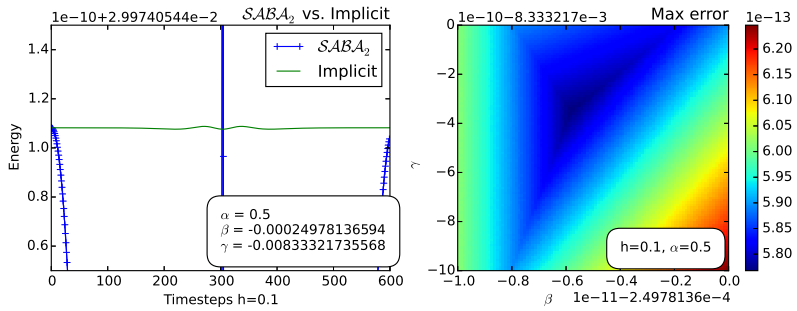

Figure 6: Search of the optimal values for β and γ. Left panel shows the oscillations of the error in the energy integral computed with values for β, γ found by the plot in the right panel. Vertical curves correspond to the numerical solution computed with $\mathcal{SABA}_2$. This is a zoomed version of the lower-right panel in Figure 5. Right panel shows the distribution of the maximal variation of the error in a small region of the $\beta-\gamma$ plane. The behaviour is equivalent for bigger and smaller regions: the minimal variation converges to a very particular region with radius around 10^{-13}.

This fact reveals an important property giving a clue on the way a numerical symplectic integrator can preserve the energy (and any other) integral in a very accurate way. The extra elements in $(\bar{Q},\bar{P})$ from (15) can be written as an approximation of the gradient vector field $\nabla_{\mathbf{z}}H(\mathbf{z}) = -J\dot{\mathbf{z}}$ considering

$$\begin{aligned}\gamma(p_i - P_i) &= -h\gamma\left(\frac{P_i - p_i}{h}\right)\\ \beta(q_i - Q_i) &= -h\beta\left(\frac{Q_i - q_i}{h}\right)\end{aligned}$$

as the approximation $hA(-J\frac{\mathbf{Z}-\mathbf{z}}{h})$ where

$$A = \begin{pmatrix} \gamma I_n & 0_n \\ 0_n & -\beta I_n \end{pmatrix}, \qquad 0_n, I_n \in M_{n\times n}(\mathbb{R}).$$

With this notation, the symplectic map (18) is redefined in terms of the numerical approximation of the gradient ∇H which belongs to the characteristic line bundle of the Hamiltonian flow

$$\frac{\mathbf{Z}-\mathbf{z}}{h} = J\nabla_z H\left(\frac{\mathbf{Z}+\mathbf{z}}{2} + hA\left(-J\frac{\mathbf{Z}-\mathbf{z}}{h}\right)\right). \tag{24}$$

In this form, the linear dependency of γ and β on h has a geometrical meaning and provides some insight into the development of an analytical expression for the matrix A, which gives us the exact flow of the Hamiltonian system. This is the subject of a companion article [15].

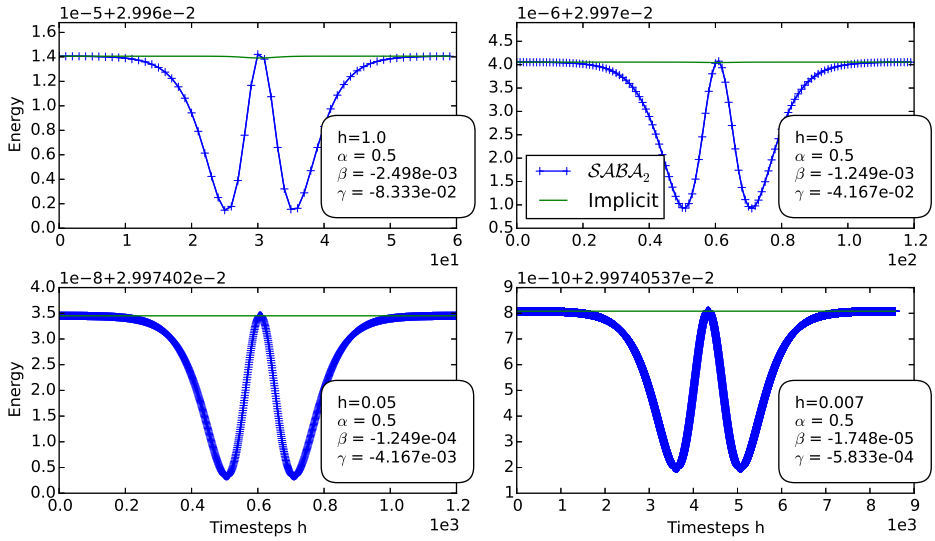

Figure 7: Energy integral of the numerical solutions of the new integrator compared to the explicit $\mathcal{SABA}_2$ integrator with initial conditions $(q_0, p_0) = (3.1, 0.0)$ and several stepsizes. For each value in the stepsize h, the values in the parameters β and γ which minimizes the oscillations in the energy integral are proportional to h. Values of those parameters for the down-right panel were extrapolated by the constants of proportionality obtained from the other panels.

5 Conclusions and perspectives

In this paper we have implemented and tested the implicit symplectic integrators constructed in [18]. This implementation considers a simple and coarse iterative process which can be refined. The main goal here was to test the accuracy of the symplectic scheme. The construction process developed in [18] opens a new point of view on generating functions and symplectic integrators owing to several new results.

i) First, we showed that gauge elements in the primitive 1-form $\theta_{\alpha,\beta,\gamma}$ enable the control of the numerical error in the energy integral and other integrals by construction. The set of parameters $\{\alpha, \beta, \gamma\} = \{\alpha_i, \beta_i, \gamma_i\}$, $i = 1, \cdots, n$ with $3n$ elements, gives the set of all possible implicit symplectic integrators passing by $\mathbf{z}$ and $\mathbf{Z}$, which are consistent with the projection (14) introduced in [18]. In the numerical tests, we searched for values of the parameters that produce the more accurate solution for the energy integral and the results are very promising.

ii) Second, numerical experiments support the existence of exact numerical sympectic integrators, contrary to Ge [11] and Ge and Marsden's [13] claims. This subject is further elaborated in a short note [15] where Ge-Marsden's claim is considered in the case of an implicit symplectic integrator. Their claim of the

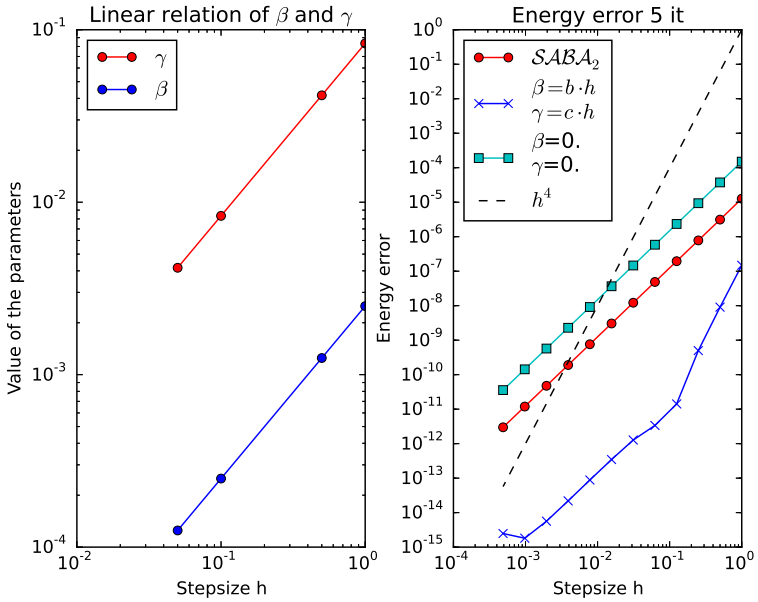

Figure 8: Left panel: The linear behaviour of the optimal values for β and γ as a function of the stepsize h. Right panel, the optimal values of β and γ for each h increase the order of the integrator up to order four.

non-existence of symplectic integrators exactly preserving the energy integral, relies on explicit symplectic maps generating the integrator. They also assume an extrapolation by Taylor series expansion. Our symplectic integrator is implicit, and the approximation is done by looking for internal points on the line's flow.

iii) Third, in the perturbed Hamiltonian pendulum, the parameters β and γ and the stepsize h satisfy a linear relationship. This fact, together with expression (24) gives a clue on the way the difference equation recovers information from the Hamiltonian formalism to produce a very accurate numerical solution. This subject is developed in [15] with a finer analysis on the symplectic transformation which better approximates the flow of a Hamiltonian vector field X_H. Other Liouvillian forms as the one obtained from the Poincaré's generating function are studied in [17].

Further work is necessary to understand the subject of symplectic integrators using Liouvillian forms. However this series of papers gives a new point of view on the subject and on the control of numerical errors in symplectic integrators.

Acknowledgements

This research was developed with support from the Fondation du Collège de France and Total under the research convention PU14150472, as well as the ERC Advanced Grant WAVETOMO, RCN 99285, Subpanel PE10 in the F7 framework.

References

[1] R. Abraham and J.E. Marsden. Foundations of mechanics Second Ed. Benjamin Cummings, 1978.

[2] S. Benenti. Linear Symplectic Relations. In Symplectic Geometry, A. Crumeyrolle and J. Grifone Eds., volume 80 of Research notes in Math. Pitman Advanced Publishing, 1983.

[3] S. Benenti. Hamiltonian Structures and Generating Functions. Springer-Verlag, 2011.

[4] E. Cartan. Leçons sur les invariants intégraux. Hermann, 1922.

[5] P.J. Channell. Symplectic Integration Algorithms, 1983.

[6] M. Chaperon. On generating families. In H. Hofer, C.H. Taubes, A. Weinstein, and E. Zehnder, editors, The Floer Memorial Volume, . Birkhäuser, 1995.

[7] C. Lubich E. Hairer and G. Wanner. Geometric Numerical Integration, Structure-Preserving Algorithms for Ordinary Differential Equations 2 Springer-Verlag, 2nd ed. edition, 2010.

[8] F. Kang and Z. Ge. On the approximation of Linear Hamiltonian Systems. J. Comput. Math., 6:88–97, 1988.

[9] W. Hua-mo Q. Meng-zhao F. Kang and W. Dao-liu. Construction of Canonical Difference Schemes for Hamiltonian Formalism Via Generating Functions. J. Comput. Math., 11:71–96, 989.

[10] Z. Ge. Generating functions, Hamilton-Jacobi equation, symplectic groupoids over Poisson manifolds. Indiana Univ. Math. J., 39:859–876, 1990.

[11] Z. Ge. Equivariant symplectic difference schemes and generating functions. Physica D, 49:376–386, 1991.

[12] Z. Ge and W. Dau-liu. On the invariance of generating functions for symplectic transformations. Diff. Geom. and its Appl, 5:59–69, 1995.

[13] Z. Ge and J. Marsden. Lie-Poisson Hamilton-Jacobi theory and Lie-Poisson integrators. Phys. Let. A, 133:134–139, 1988.

[14] L. Hörmander. Fourier integral operators I. Acta Math., 127:79–183, 1971.

[15] Jiménez-Pérez, H. Exact symplectic integrators from Liouvillian forms. in progress, 2015.

[16] Jiménez-Pérez, H. Geometrization of symplecticity conditions for implicit schemes. in progress, 2015.

[17] Jiménez-Pérez, H. On the Poincaré's generating function and the symplectic mid-point integrator. in progress, 2015.

[18] Jiménez-Pérez, H. Symplectic maps: from generating functions to Liouvillian forms. preprint, 2015.

[19] F. Kang. Difference schemes for Hamiltonian Formalism and Symplectic Geometry. J. Comput. Math., 4:279–289, 1985.

[20] F. Kang. On Difference Schemes and Symplectic Geometry. In K Feng, editor, 1984 Beijing Symp Diff Geometry and Diff Equations, pages 42–58, 1985.

[21] F. Kang and M. Qin. Symplectic Geometric Algorithms for Hamiltonian Systems. Springer-Verlag, 2012.

[22] J. Laskar and P. Robutel. High order symplectic integrators for perturbed Hamiltonian systems. Celestial Mechanics and Dynamical Astronomy, 80:39–62, 2001.

[23] C.-M. Libermann, P., Marle. Symplectic Geometry and Analytical Mechanics. Ridel, 1987.

[24] T.S. Marsden, J.E., Ratiu. Introduction to Machanics and Symmetry. Springer-Verlag, 1999.

[25] V.P. Maslov. Theorie des perturbations et methodes asymptotiques, (French version from the Russian ed Dunod, 1972.

[26] C.R. Menyuk. Some Properties of the Discrete Hamiltonian Method. Physica D, 11:109–129, 1984.

[27] Miesbach S. and H.J. Pesch. Symplectic phase flow approximation for the numerical integration of canonical systems. Numer. Math., 61:501–521, 1992.

[28] P. Libermann. On Liouville Forms. Poisson Geometry, Banach Center Publications, 51:151–164, 2000.

[29] Scovel C. P.J., Channell. Symplectic Integration of Hamiltonian Systems. Nonlinearity, 3:231–259, 1990.

[30] H. Poincaré. Les méthodes nouvelles de la mécanique céleste Tome III, volume III. Gauthier-Villars, 1899.

[31] R. Ruth. A Canonical Integration Technique. IEEE Trans. Nucl. Sci., 30:2669–2671, 1983.

[32] J.M. Sanz-Serna. Runge-Kutta Schemes for Hamiltonian Systems. BIT, 28:877–883, 1988.

[33] C. L. Siegel. Symplectic Geometry. American Journal of Mathematics, 65:1–86, 1943.

[34] C. L. Siegel. Symplectic Geometry. Academic Press, 1964.

[35] J. Sniatycki and W.M. Tulczyjew. Generating forms on Lagrangian submanifolds. Indiana Univ. Math. J, 22, 1972.

[36] W.M. Tulczyjew. The Legendre Transformation. Annales de l'IHP, section A:1, 101-114.

[37] C. Viterbo. Symplectic topology as the geometry of generating functions. Mathematische Annalen, 292:685–710, 1992.

[38] R. De Vogelaere. Methods of Integration which Preserve the Contact Transformation Property of the Hamiltonian Equations, 1956.

[39] A. Weinstein. The invariance of Poincaré's generating function for canonical transformations. Inventiones mathematicae, 16:202–213, 1972.

[40] W.M. Tulczyjew. Les sous-variétés lagrangiennes et la dynamique lagrangienne. C.R.Acad.Sci. Paris, 283:675–678, 1976.

[41] H. Xue and A. Zanna. Generating functions and volume preserving mappings. Disc. and Cont. Dyn. Syst, 34:1229–1249, 2014.